UNCLASSIFIED

AD NUMBER

AD482692

NEW LIMITATION CHANGE

TO

Approved for public release, distribution unlimited

FROM

Distribution authorized to U.S. Gov't. agencies and their contractors; Critical Technology; May 1966. Other requests shall be referred to US Army Electronics Command, Attn: AMSEL-KL-TM, Ft. Monmouth, NJ.

AUTHORITY

US Army Electronics Command ltr dtd 16 Jun 1971

THIS PAGE IS UNCLASSIFIED

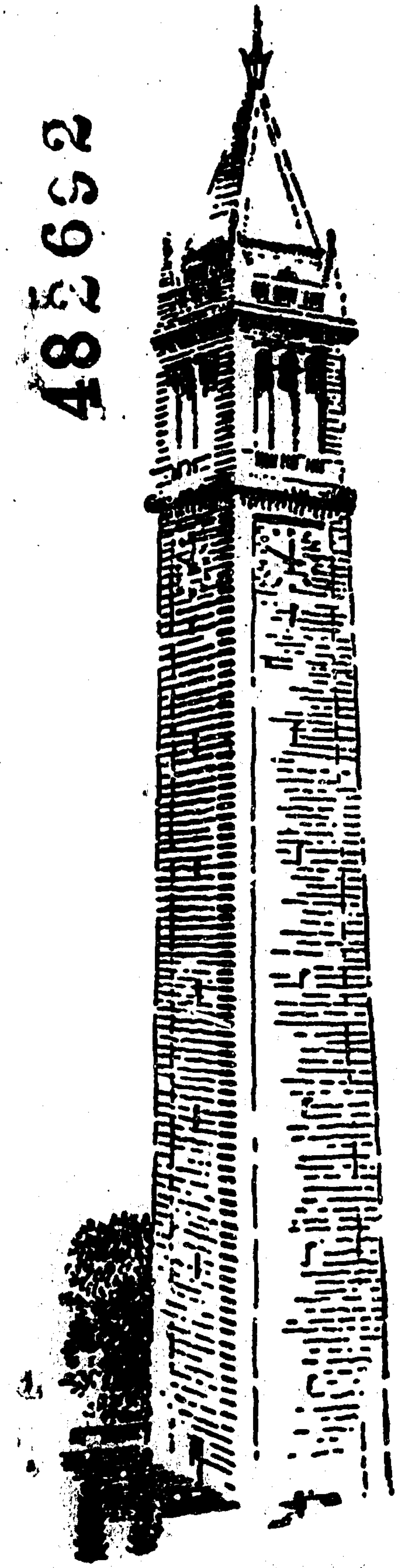

STUDY OF CROSSED-FIELD AMPLIFIERS

Report Nr. 10
Contract Nr. DA 36-039 AMC-02164(E)

Tenth Quarterly Progress Report
16 September - 15 December 1965

This document is subject to special export controls and each transmittal to foreign governments or foreign nationals may be made only with prior approval of CG, U. S. Army Electronics Command, Ft. Monmouth, N. J. Attn: AMSEL-KL-TM

United States Army Electronics Command
Fort Monmouth, New Jersey

ELECTRONICS RESEARCH LABORATORY

College of Engineering

University of California, Berkeley

Request for additional copies by Agencies of the Department of Defense, their contractors and other Government agencies should be directed to the:

DEFENSE DOCUMENTATION CENTER (DDC)
CAMERON STATION
ALEXANDRIA, VIRGINIA 22314

Department of Defense contractors must be established for DDC services or have their "need-to-know" certified by the cognizant military agency of their project or contract.

NOTICES

Disclaimers

The findings in this report are not to be construed as an official Department of the Army position, unless so designated by other authorized documents.

The citation of trade names and names of manufacturers in this report is not to be construed as official Government indorsement or approval of commercial products or services referenced herein.

Disposition

Destroy this report when it is no longer needed. Do not return it to the originator.

STUDY OF CROSSED-FIELD AMPLIFIERS

Tenth Quarterly Progress Report
16 September - 15 December 1965
Contract Nr. DA 36-039 AMC-02164(E)

United States Army Electronics Command
Fort Monmouth, New Jersey

ABSTRACT

An electron gun in which the cathode and accelerating regions are shielded from the magnetic field of the drift region is proposed. Beam synthesis techniques are utilized to obtain electrode configurations which produce a nearly laminar beam. Second order corrections to the beam synthesis method are found to be insignificant for the case of a large cathode width. Expression for the minimum noise figure of crossed-field amplifiers is derived and its dependence on the space-charge parameter is shown.

The parametric dependence of the noise figure of crossed-field microwave amplifiers was established theoretically and experimentally. Conditions for the low-noise operation of crossed-field amplifiers were obtained. The dependence of space-charge smoothing factor as a function of cycloid length to cathode length is estimated from the theoretical study of the crossed-field potential minimum region.

The study of certain crossed-field effects in solids was initiated.

TABLE OF CONTENTS

ABSTRACT	iii
SHIELDED-GUN LOW-NOISE AMPLIFIER	1
1. Transition from Kino Flow to Brillouin Flow	2
2. Design of the Shielded-Gun	2
3. Synthesis of the Beam	7
NOISE-FIGURE STUDIES ON FORWARD-WAVE CROSSED-FIELD AMPLIFIER	13
BACKWARD-WAVE NOISE-FIGURE STUDIES	21
CATHODE REGION STUDIES	23
SECOND-ORDER CORRECTIONS TO THE FIRST-ORDER CROSSED FIELD SHEET BEAM FLOW	29
CROSSED-FIELD INTERACTIONS OF EM AND SOUND WAVES WITH CURRENT CARRIERS IN SOLIDS	30

ELECTRONICS RESEARCH LABORATORY

University of California
Berkeley, California

Quarterly Progress Report
15 December 1965

Study of Crossed-Field Amplifiers
DA 36-039 AMC-02164(E)

This report presents progress on research in crossed-field amplifiers for the quarter ending 15 December 1965. Major stress has continued on the understanding and improvement of noise processes in backward-wave and forward-wave crossed-field amplifiers. The beam synthesis method, which has been so successful on unshielded guns, has been applied to guns which are shielded from the magnetic field. Second-order effects have been applied to the synthesis method, and the cathode region has been studied with emphasis on the feedback effect of returned electrons. Calculations of the noise figures of amplifiers with velocity jumps have been completed. The companion experimental and theoretical study designed to reveal the effect of key parameters on the noise figure has also been c .npleted and is now being prepared for publication.

During this report period, stress has also been placed on the task concerned with extending some of the above techniques to charge carriers in solids. Several possible effects have been reviewed in detail, and additional review is continuing. Current stress, however, is on the amplification of the fast cyclotron wave of a helicon configuration, or of the Alfven wave in an orthodox crossed-field configuration.

SHIELDED-GUN LOW-NOISE AMPLIFIER

(R. A. Rao, Professor T. Van Duzer, and Dr. S. P. Yu)

The objective of this project is to design a low noise shielded-gun amplifier and measure its noise characteristics.

1. Transition from Kino Flow to Brillouin Flow

As described in ERL Semiannual Progress Report No. 1, a method has been developed for synthesizing crossed-field electron guns. It has been used to synthesize an electron gun which produces a beam with Kino flow characteristics near the cathode and Brillouin flow characteristics in the drift region. The tube has been fabricated and tested. The operating characteristics of the tube agree very well with the theory reported earlier.

2. Design of the Shielded-Gun

Experiments of Astrom [1], Guenard and Huber [2], Little, Ruppel and Smith [3], Sato [4], and Rao [5] indicate the presence of high negative-sole currents and very high equivalent temperatures of electrons in crossed-field amplifiers. The same experiments show that the beam has a high r.f. noise current which increases when the cathode is operated under space-charge-limited conditions. This behavior of the M-type beam, as contrasted with the O-type beam, may be explained by the fact that the noise transport in the potential minimum region is different when there is a crossed magnetic field in the potential minimum region. Thus, it is considered that a careful study

---

[1] E. Astrom, "Electrons in High Vacuum in Strong Magnetic Fields," Proc. Conference on Dynamics of Ionized Media, (London), (April 1951).

[2] P. Guenard and H. Huber, "Etude Experimentale de l'interaction par Ondes de Charge d'espace au sein d'un Faisceau Electronique se Deplacant dans des Champs Electrique et Magnetique Croises," Annales de Radio-electricite', 7, pp. 252-278, (Oct. 1952).

[3] R. P. Little, H. M. Ruppel and S. T. Smith, "Beam Noise in Crossed Electric and Magnetic Fields," J. Appl. Phys., 29, p. 1376, (Sept. 1958).

[4] T. Sato, "An Experimental Investigation of Crossed-Field Interaction," Stanford University Electronics Research Laboratory, TR-No. 385-5, (Feb. 1960).

[5] R. A. Rao, "Noise in Crossed-Field Guns," M. S. Thesis, University of California, Berkeley, (June 1961).

of the noise performance of a crossed-field amplifier in which the cathode is shielded from the magnetic field may throw some light on the high noise in M-type beams. Very recently, Mantena and Van Duzer [6], and Wadhwa and Van Duzer [7] obtained low noise figures in M-type amplifiers without shielding the cathode region from the magnetic field. This result seems to reduce the importance of having the magnetic field in the cathode region. However, these results have been obtained for a particular type of beam (Kino short-gun beam), and beams of other types (Kino long-gun beam) are known to be very noisy. The problem of noise in crossed-field beams has not been completely solved, and it is felt that there is a great deal to be learned by studying the effect of shielding the cathode region from the magnetic field on the noise characteristics of a crossed-field beam.

The cathode region in our model will be enclosed in a hollow prolate spheroid immersed with its major axis along the direction of the applied magnetic field. If the permeability of the material is high, the magnetic field inside the spheroid will be negligibly small and will approximate the situation of perfect magnetic shielding quite well. The presence of the magnetic spheroid makes the magnetic field highly non-uniform in the neighborhood of the spheroid. Before the beam and the gun may be synthesized, one should calculate the magnetic field in and about the hollow spheroid. The problem is to solve Laplace's equation with the proper boundary conditions at infinity and on the two surfaces of the hollow spheroid. A more general case of a hollow ellipsoid will be solved by using ellipsoidal coordinates, and by taking the limit when the two minor axes are equal we obtain the results for the hollow spheroid. We refer to Fig. 1.

---

[6] N. R. Mantena and T. Van Duzer, "Crossed-Field Backward-Wave Amplifier Noise-Figure Studies," J. Electronics and Control, 17, pp. 497-511, (Nov. 1964).

[7] R. P. Wadhwa and T. Van Duzer, "A 3.5 db Noise-Figure, S-Band, Medium Power, Forward-Wave, Injected Beam Crossed-Field Amplifier," Proc. IEEE, 53, pp. 425-426, (April 1965).

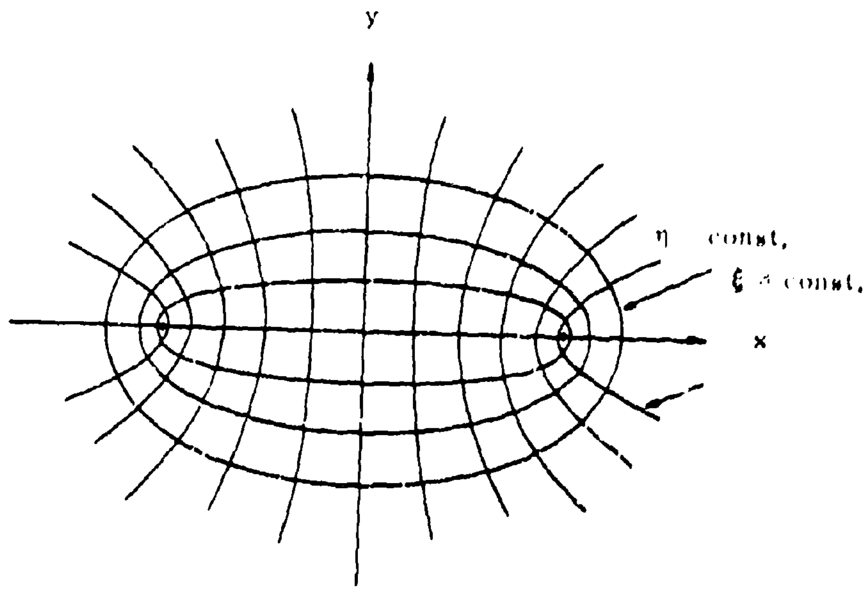

Fig. 1 . Ellipsoidal coordinates

In ellipsoidal coordinates, Laplace's equation may be written as

$$\nabla^2\psi = \frac{4}{(\xi - \eta)(\xi - \zeta)(\eta - \zeta)} \left[(\eta - \zeta) R_\xi \frac{\partial}{\partial \xi}\left(R_\xi \frac{\partial \psi}{\partial \xi} \right) \right.$$

$$\left. + (\zeta - \xi) R_\eta \frac{\partial}{\partial \eta}\left(R_\eta \frac{\partial \psi}{\partial \eta} \right) + (\xi - \eta) R_\zeta \frac{\partial}{\partial \zeta}\left(R_\zeta \frac{\partial \psi}{\partial \zeta} \right) \right] = 0, \qquad (1)$$

where ξ = constant, η = constant, and ζ = constant are the level surfaces of confocal ellipsoids, hyperboloids of one sheet, and hyperboloids of two sheets, respectively, and ψ is the magnetic potential function.

$$R_s = \sqrt{(s + a^2)(s + b^2)(s + c^2)} \;, \qquad (s = \xi,\ \eta,\ \zeta). \qquad (2)$$

Two linearly independent solutions for this equation are derived by Stratton [8]:

$$\psi_1 = F(\xi)\ F(\eta)\ F(\zeta), \qquad (3)$$

$$\psi_2 = G(\xi)\ F(\eta)\ F(\zeta), \qquad (4)$$

where

$$F(s) = \sqrt{s + a^2} \;, \qquad (s = \xi,\ \eta,\ \zeta), \qquad (5)$$

and

$$G(\xi) = \int_\xi^\infty \frac{d\xi}{(\xi + a^2)\ R_\xi} \;. \qquad (6)$$

The permeabilities of regions I, II, and III of Fig. 2 are μ_0, $\mu_0\mu$, and μ_0, respectively. The outer surface of the hollow ellipsoid is $\xi = 0$, and the inner surface is taken to be $\xi = -\alpha^2$.

---

[8] J. A. Stratton, Electromagnetic Theory, McGraw-Hill Book Co., New York, N. Y., p. 209, June 1941.

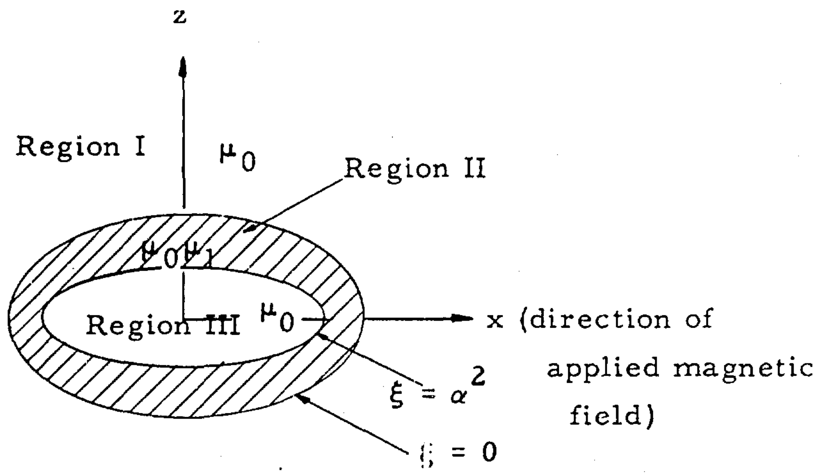

Fig. 2. Cross-section of hollow spheroid in x-z plane

The solutions in the three regions may be written as linear combinations of the solutions represented by Eqs. (3) and (4).

$$\psi_1 = F(\eta)\, F(\zeta)\, [c_1\, F(\xi) + c_2\, G(\xi)], \tag{7}$$

$$\psi_2 = F(\eta)\, F(\zeta)\, [c_3\, F(\xi) + c_4\, G(\xi)], \tag{8}$$

and

$$\psi_3 = c_5\, F(\xi)\, F(\eta)\, F(\zeta)\,. \tag{9}$$

These solutions are chosen so that the magnetic field is finite everywhere and becomes uniform at infinity. There are five boundary conditions: one at infinity, and two each at $\xi = 0$ and $\xi = -\alpha^2$ for the magnetic scalar potential and normal field. Thus, the five constants c_1, c_2, c_3, c_4, and c_5 may be determined. The limit may be taken as $c \to b$ so that the elipsoid becomes a hollow spheroid.

The magnetic field lines are plotted in Fig. 3 in the x-z plane. For the case illustrated in the figure, the major axis of the outer spheroidal surface is 2 in., the minor axis is 0.6 in., the wall thickness is 0.1 in., and the permeability of the material of the box is chosen to be 1000.

3. Synthesis of the Beam

One of the considerations in the design of the gun is to make it short so that the diocotron gain in the gun region is small. This requires that the region over which the magnetic field is nonuniform is small; hence, the dimensions of the shielding box should be small. Since the cathode and some of the focusing electrodes will be inside the shield, it is necessary to compromise. The dimensions chosen above are a result of this compromise. To obtain a good understanding of the problems involved in the synthesis of the beam in a nonuniform magnetic field, a very simple model is chosen first. The beam is assumed to emanate from a strip cathode with its shorter side along the y-axis and its longer side along the direction of the applied magnetic field. The problem is solved entirely in the y-z plane with the assumption that the beam is infinite in the direction of the magnetic field. The beam is assumed to be thin so that the magnetic field along the beam edges is substantially the same as along the axis of the beam and the paraxial-ray equation may be used in the synthesis of the beam. In the y-z plane, the magnetic field is entirely x-directed. The paraxial-ray equation is given by

$$2\phi_0 r'' + \phi_0' r' + (\phi_0'' + 4k_0^2 \phi_0 + 2k_0 |b| \sqrt{2\eta\phi_0} + \eta b^2) r = \frac{I}{2w\epsilon_0 \sqrt{2\eta\phi_0}}, \qquad (10)$$

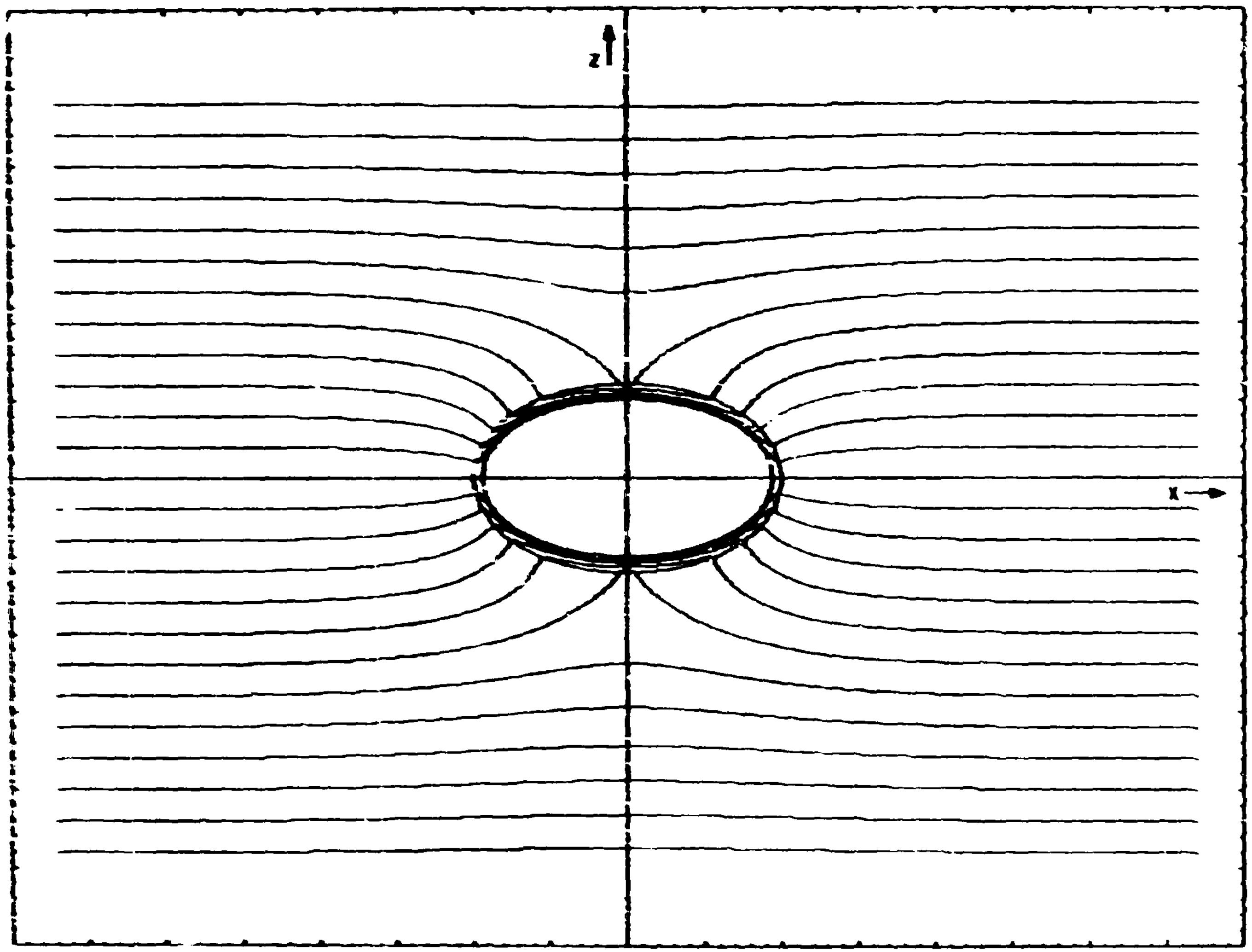

Fig. 3. Magnetic field lines in the x-z plane.

where

ϕ_0 = potential along the axis of the beam,

r = curvature measured along the axis of the beam,

b = magnetic field measured along the axis of the beam,

I = total current in the beam,

w = length of the cathode in the direction of the magnetic field,

ϵ_0 = permittivity of free space, and

η = charge to mass ratio of an electron.

The primes indicate differentiation with respect to the arc length along the axis of the beam. The only difference between this equation and that used to synthesize a beam in a uniform magnetic field is that the value of the magnetic field is assumed to be a function of the arc length s in the present case. It is convenient to use the following set of normalizations.

$$\omega_c = \eta b_0 , \tag{11}$$

$$B = \frac{b}{b_0} , \tag{12}$$

$$X = \frac{\epsilon_0 \omega_c^3}{\eta J_k} x , \tag{13}$$

$$\Phi = \frac{\epsilon_0^2 \omega_c^4}{\eta J_k^2} \phi , \tag{14}$$

$$\Psi = \frac{\epsilon_0 \omega_c^2}{J_k} \psi , \tag{15}$$

where

b_0 = applied magnetic field,

J_k = current density at the cathode,

ϕ = electrostatic potential along the axis of the beam, and

ψ = scalar magnetic potential.

Using these normalizations and assuming that the normalized cathode half-thickness is unity, we can reduce the paraxial ray equation to

$$2\Phi_0 R'' + \Phi_0 R' + \left[\Phi_0'' + 4K_0^2 \Phi + 2|B|K_0\sqrt{2\Phi_0} + B^2\right]R = \frac{1}{\sqrt{2\Phi_0}} . \tag{16}$$

The auxiliary equation for the off-axis potential is

$$\Phi(R, S) = \Phi_0(s) + A_1 R + A_2 R^2 , \tag{17}$$

where

$$A_1 = 2\Phi_0 K_0 + |B|\sqrt{2\Phi_0} + \frac{1}{2\sqrt{2\Phi_0}} , \tag{18}$$

$$A_2 = -\frac{1}{2}\left[\Phi_0'' - 2K_0^2 \Phi_0 - |B| K_0\sqrt{2\Phi_0}\right] . \tag{19}$$

Equations (16) and (17) are used as the basis for synthesizing the beam. Inside the shield, the magnetic field is small and uniform and Kino flow is used from the cathode up to a plane half-way to the wall of the shielding box. As a first step, the regions inside and outside the shielding box are assumed to be electrically isolated and the beam is synthesized by working from the cathode to the wall of the shielding box inside the box and working from the drift region to the wall of the

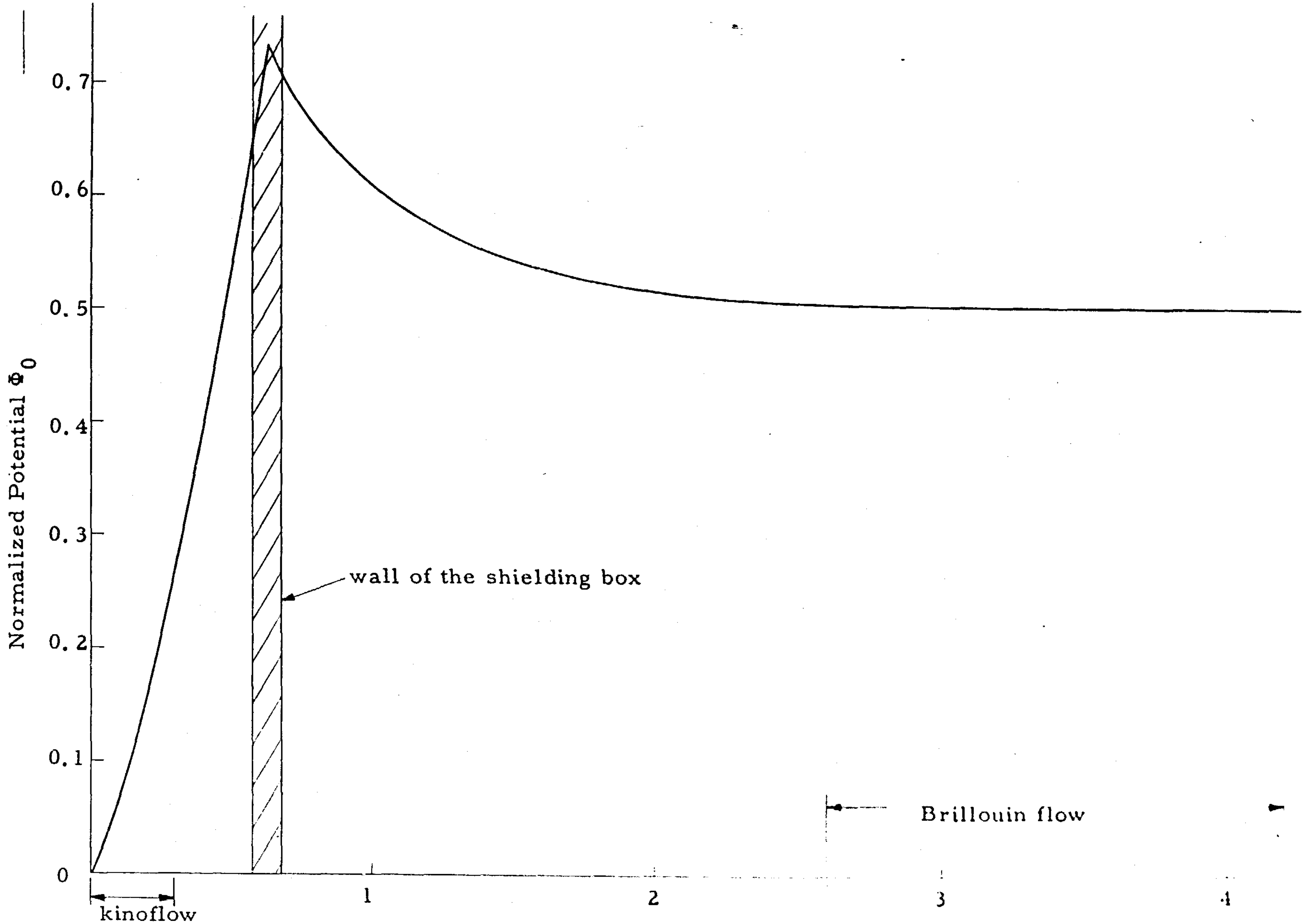

Fig. 4. Axial potential for shielded-gun beam.

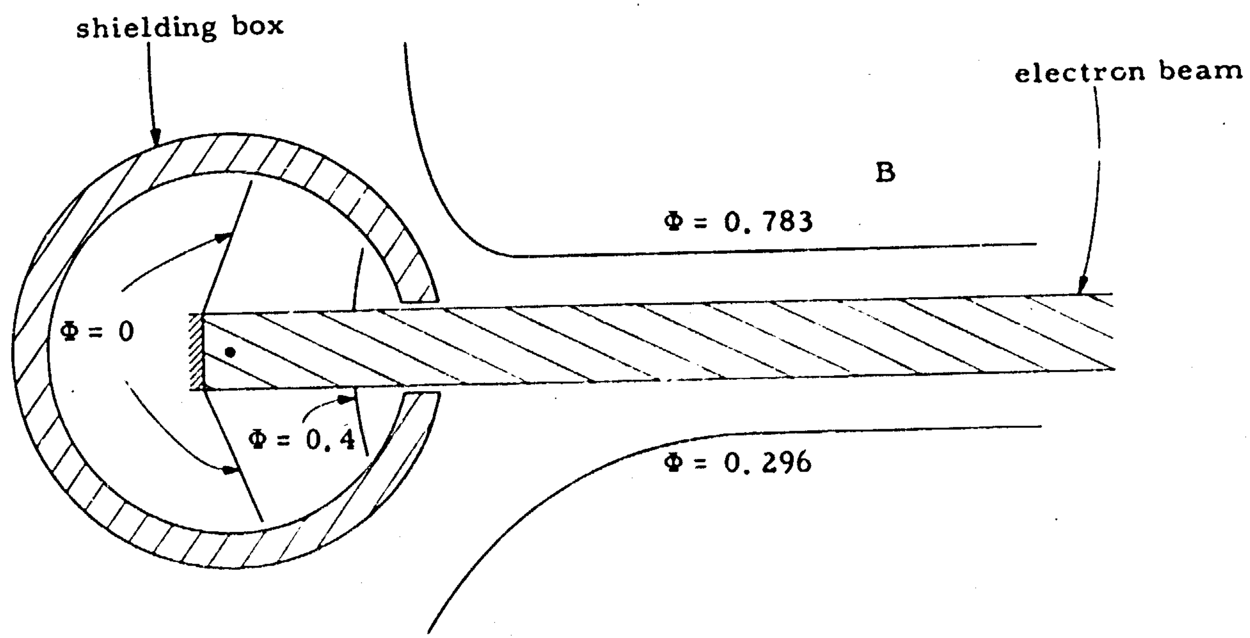

Fig. 5. Electron beam and electrodes for shielded-gun.
(The potentials shown here are normalized values.)

shielding box outside the shielding box. For a beam of constant thickness, the axial potential obtained this way is shown in Fig. 4. The electric fields along the beam edges calculated from Eq. 17 show sharp discontinuities across the wall of the shielding box. The electrodes are designed separately inside and outside the box using analytic continuation. Figure 5 shows the shapes of the electrodes and the beam for this particular model.

Design of the shielded-gun will be continued in the next report.

NOISE-FIGURE STUDIES ON FORWARD-WAVE CROSSED-FIELD AMPLIFIER

(A. Sasaki and Professor T. Van Duzer)

The aim of this work is to develop understanding of the noise characteristics of forward-wave crossed-field amplifiers to a sufficient degree to permit appreciable noise-figure reductions. The normal-mode approach will be used in the study of noise transducing schemes.

In continuing the minimum noise-figure studies, we now introduce the self-power density spectrum (SPDS) and the cross-power density spectrum (CPDS) of noise defined as

$$\left.\begin{aligned} \Phi_T &= \frac{\frac{1}{2}\overline{U_T(\omega)^2}}{4\pi\,\Delta f}, & \Phi_L &= \frac{\frac{1}{2}\overline{U_L(\omega)^2}}{4\pi\,\Delta f} \\ \Psi_T &= \frac{\frac{1}{2}\overline{I_T(\omega)^2}}{4\pi\,\Delta f}, & \Psi_T &= \frac{\frac{1}{2}\overline{I_L(\omega)^2}}{4\pi\,\Delta f} \end{aligned}\right\} \qquad (1)$$

and

$$
\left.
\begin{aligned}
\theta_1 &= \frac{\frac{1}{2}\,\overline{U_T(\omega)\,U_L(\omega)^*}}{4\pi\,\Delta f} & \theta_2 &= \frac{\frac{1}{2}\,\overline{U_T(\omega)\,I_T(\omega)^*}}{4\pi\,\Delta f} \\
\theta_3 &= \frac{\frac{1}{2}\,\overline{U_T(\omega)\,I_L(\omega)^*}}{4\pi\,\Delta f} & \theta_4 &= \frac{\frac{1}{2}\,\overline{U_L(\omega)\,I_T(\omega)^*}}{4\pi\,\Delta f} \\
\theta_5 &= \frac{\frac{1}{2}\,\overline{U_L(\omega)\,I_L(\omega)^*}}{4\pi\,\Delta f} & \theta_6 &= \frac{\frac{1}{2}\,\overline{I_L(\omega)\,I_T(\omega)^*}}{4\pi\,\Delta f}
\end{aligned}
\right\} \qquad (2)
$$

where the bar represents the mean-squared value, and Δf is the bandwidth of the amplifier. The CPDS is complex and may be written as

$$
\theta_n = \Pi_n + j\Lambda_n \,. \qquad (3)
$$

To express Eq. (7) in the last quarterly report in terms of SPDS and CPDS, we use the matrix W whose elements are SPDS and CPDS:

$$
W = \lim_{T\to\infty} \frac{\pi}{2T}\,\overline{w(\omega)\,w(\omega)^{\dagger}}\,, \qquad (4)
$$

where the bar represents the ensemble average for the time interval T and the superscript $\dagger$ denotes the Hermitian conjugate. The ensemble average and the mean-squared average are related by

$$
\lim_{T\to\infty} \frac{2\pi}{T}\,\overline{X(\omega)\,X(\omega)^*} = \frac{\overline{X(\omega)\,X(\omega)^*}}{4\pi\,\Delta f}\,,
$$

where $X(\omega)$ is a Fourier component of noise fluctuations at the angular frequency ω. Using Eq. (9) derived in the last quarterly report, we obtain the useful matrix equation for finding the invariant noise parameters:

$$M^{-1} W_b R M = W_a R . \qquad (5)$$

This is a similarity transformation of the matrix WR, so the trace and determinant of WR are invariant. Expressing those invariant noise parameters in terms of the SPDS and CPDS of the normal-mode amplitudes, we have

$$\frac{1}{2} \text{trace (WR)} \equiv \Pi_i = (A_{ff} - A_{ss}) + j(A^*_{gd} - A_{gd}) , \qquad (6)$$

where A_{ff} is called the SPDS of the fast cyclotron wave defined as

$$A_{ff} = \frac{a_f(\omega)\, a_f(\omega)^*}{4\pi\, \Delta f} , \qquad (7)$$

and the other terms follow the same definition. Here the subscripts s, g, and d denote the slow cyclotron, the growing space-charge, and the decaying space-charge waves, respectively. The invariant parameter Π_i represents the kinetic power of the electron beam due to the noise fluctuations and corresponds to the parameter Π in an O-type amplifier. For the sake of simplicity, only the case of zero correlation is discussed here. The invariant noise parameter S_i for the zero correlation case is given by

$$\det(WR) \equiv S_i^4 = 2^4 (A_{ff}^2 - A_{ss}^2) \{(A_{ff}^2 - A_{ss}^2) - \frac{1}{\alpha}(A_{ff} + A_{fs})(A_{gg} + A_{gd})$$

$$- \alpha(A_{ff} - A_{fs})(A_{gg} - A_{gd}) + (A_{gg}^2 - A_{gd}^2)\} , \qquad (8)$$

which is equivalent to the parameter S in an O-type amplifier.

We use the beam model in which the reference plane beyond the potential minimum is followed by a drift region where the dc velocity of the beam is much larger than the magnitude of the fluctuations of velocity. This is not a restriction on the generality of our results as far as we use the invariant noise parameters of the linear and lossless region. It must be mentioned that the diocotron effect does not prevent the region being represented by a linear and lossless transducer. Thus, the invariant noise parameters, calculated at the reference plane, are not affected by the diocotron effect. The neglection of an accelerating region does not affect the parameters since that region is assumed to be lossless and linear. However, it can be considered that the dioctron effect exists in the accelerating region. The noise-figure expression contains the diocotron effect as will be shown later. Therefore, the drift length of the beam model for the analysis must be chosen to express the diocotron effect of an actual amplifier. In other words, the drift length, d, of the beam model is not the same as the drift length in an amplifer, but is an equivalent length for expressing the diocotron effect of the accelerating and drift regions.

The noise-figure expression is

$$NF = 1 + \frac{4\pi}{kT} \frac{1}{|G_{65}|^2} \left\{ \left| G_{6g} \, e^{\beta_s d} \right|^2 A_{gg} + \left| G_{6d} \, e^{-\beta_s d} \right|^2 A_{dd} + \left(G_{6g} G_{6d}^* A_{gd} + G_{6g}^* G_{6d} A_{gd}^* \right) \right\} , \qquad (9)$$

where we have assumed synchronization of phase velocity between the circuit wave and the space-charge waves and impedance matching to the output circuit. Here the gain parameter G_{6g} is defined as

$$G_{6g} = \left. \frac{c_6(\omega)}{b_g(\omega)} \right|_{b_f = b_s = b_g = b_5 = 0} ,$$

where the $c(\omega)$ expresses the normal-mode amplitude at the output plane, the $b(\omega)$ at the input plane. The subscripts 5 and 6 denote the input plane and the output plane of the circuit, respectively. The SPDS and CPDS of normal-mode amplitudes in Eq. (9) are those at the reference plane. The noise-figure expression given by Eq. (9) is written as

$$NF = 1 + \frac{4\pi}{kT|G_{65}|^2} \left\{ \left(\left|G_{6g}\, e^{\beta_s d}\right|^2 + \left|G_{6d}\, e^{-\beta_s d}\right|^2 \right) A_{gg} \right.$$

$$\left. + \left(G_{6g} G^*_{6d} + G^*_{6g} G_{6D} \right) A_{gd} \right\}, \tag{10}$$

where we notice that A_{gd} is real and $A_{gg} = A_{dd}$ for the zero correlation case.

To find the minimum noise-figure expression in the present case, we minimize the noise-figure expression (10) by the usual mathematical procedure, that is, we minimize the equation subject to the condition of a constant value of S_i since the other parameter Π_i is zero in the zero correlation case. We obtain the minimum noise-figure expression:

$$NF_{min} = 1 + \frac{2\pi}{kT|G_{65}|^2}\, 2S_i \cdot$$

$$\cdot \sqrt{\left\{ j\left(G_{6g} G^*_{6d} - G^*_{6g} G_{6d} \right) \right\}^2 + \left(\left|G_{6g}\, e^{\beta_s d}\right|^2 - \left|G_{6d}\, e^{-\beta_s d}\right|^2 \right)^2}. \tag{11}$$

It is desirable to express the equation in practical terms rather than the gain parameters. Solving the coupled-mode equations which are valid for the centered beam in the case of the space-charge wave amplifier, we obtain,

$$
\left.\begin{aligned}
|G_{6g}|^2 &= \frac{G}{2}\left(1 - \frac{1}{G}\right)\left(2S_g^2 + 1 + 2S_g\sqrt{S_g^2 + 1}\right), \\
|G_{6d}|^2 &= \frac{G}{2}\left(1 - \frac{1}{G}\right)\left(2S_g^2 + 1 - 2S_g\sqrt{S_g^2 + 1}\right),
\end{aligned}\right\} \qquad (12)
$$

and

$$
S_g^2 = S^2 \frac{\sqrt{G} - 1}{\sqrt{G} + 1} ,
$$

where S is the space-charge parameter and $G = |G_{65}|^2$, the power g gain of an amplifier. We have the equation†

$$
-j\left(G_{6g}^{*} G_{6d} - G_{6g} G_{6d}^{*}\right) + |G_{65}|^2 = 1 , \qquad (13)
$$

which must be satisfied in a crossed-field amplifier. The substitution of Eqs. (12) and (13) into Eq. (11) gives

$$
NF_{min} = 1 + \frac{2\pi}{kT} S_i\left(1 - \frac{1}{G}\right)\left(2\sqrt{1 + f^2(S)}\right) , \qquad (14)
$$

where

$$
f(S) = 2S_g\sqrt{S_g^2 + 1} \quad \cosh 2\beta_s d + (2S_g^2 + 1) \sinh 2\beta_s d . \qquad (15)
$$

† Semiannual Progress Report No. 2, Electronics Research Lab., University of Calif., Berkeley, Dec. 31, 1965.

Expression (14) can be applied to either the forward- or backward-wave amplifier, because Eqs. (12) and (13) are valid for both types. Expression (7) is similar to the minimum noise-figure expression for an O-type amplifier, except for the last term in Eq. (7).

The dependence of minimum noise figure on the space-charge parameter S can be seen to be simplified in Eq. (14) by assuming zero drift length d = 0 and a high gain G >> 1.

$$NF_{min} = 1 + \frac{2\pi}{kT} S_i \{2(2S^2 + 1)\} . \qquad (16)$$

To reduce the noise figure, Fig. 6, the space-charge parameter must be smaller as shown in the figure and the drift length must be shorter as given by Eq. (11). The decrease of noise figure due to decreasing space charge can be understood in the following way. When space charge is decreased, the wave properties of the two space-charge waves become similar since the space-charge effects cause splitting of the degeneracy of space-charge waves in crossed fields. The gain parameters of two waves become close as can be seen in Eq. (12), which gives the smaller value of Eq. (5). In other words, two similar waves cancel their noise fluctuations when the conditions for the minimization are satisfied. The decrease of noise figure due to decreasing space charge is true not only for the minimum noise figure but also for a general expression (10) of noise figure. The decrease of noise figure for a general case is due to the reduction of the diocotron effect. During the next report period, the effect of the correlation terms on the minimum noise-figure expression will be examined.

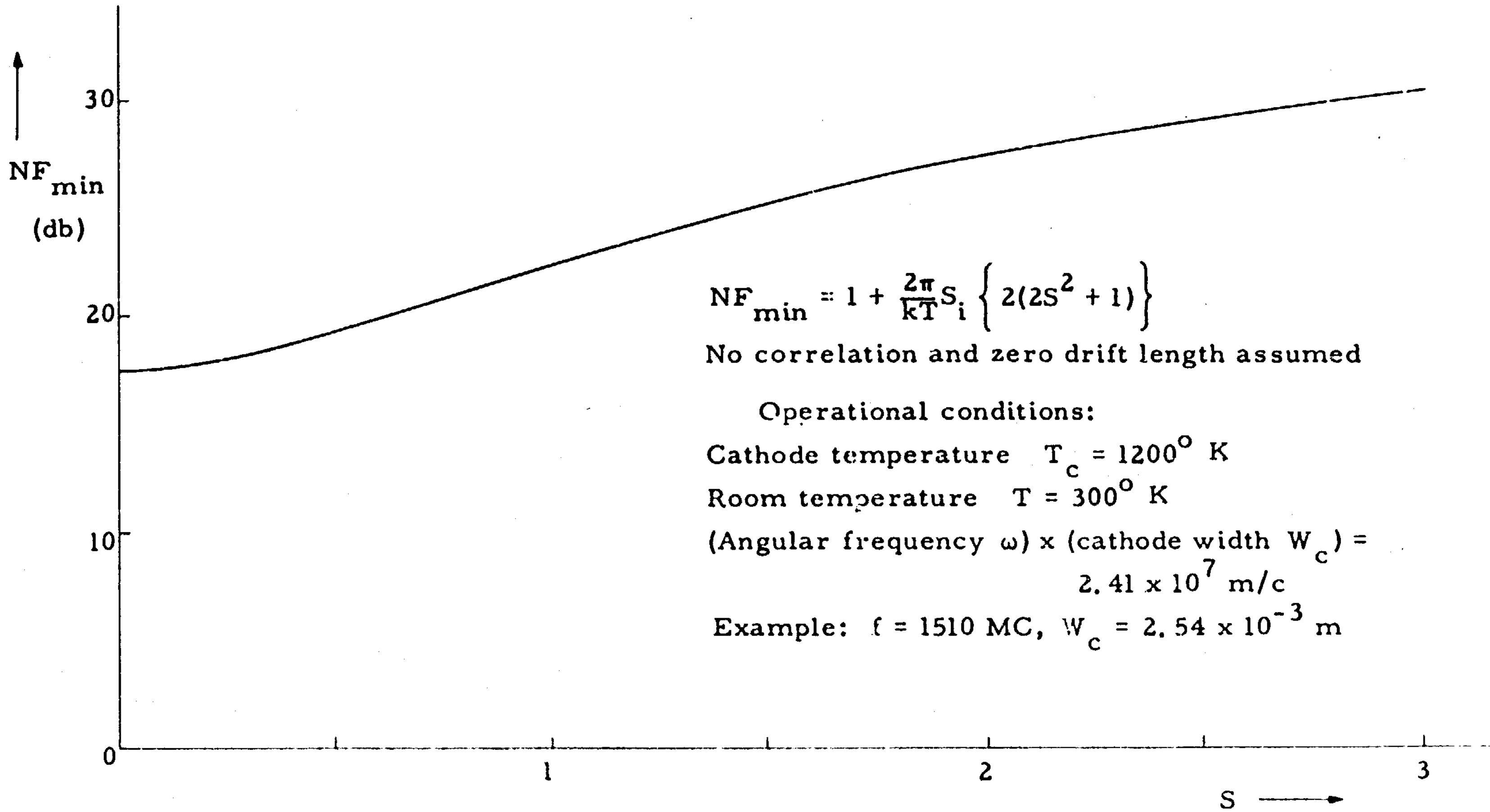

Fig. 6. Dependence of minimum noise figure on space-charge parameter S

BACKWARD-WAVE NOISE-FIGURE STUDIES

(N. R. Mantena, Professor T. Van Duzer, and Dr. S. P. Yu)

The objective of this research has been to determine the specific parametric dependence of the noise-figure of crossed-field microwave amplifiers and to establish conditions for the low-noise operation of these amplifiers. This goal has been achieved and a final report has been prepared. The report will be published by ERL in early 1966. A summary of the report follows.

Summary

Over the past decade a great deal has been said in the literature about inherent noise of crossed-field microwave amplifiers. The present investigation is concerned with the noise-figure dependence of crossed-field amplifiers on the various parameters of the gun region, drift space, and the interaction region. The establishment of parametric dependence is an essential next step in crossed-field noise work leading to the design of very low noise-figure amplifiers.

The analytical parts of this work are based on a model proposed by Van Duzer. The fluctuation quantities at the cathode are transformed through the accelerating region by using Van Duzer's transformation equations for the crossed-field diode. The 4×4, drift-region, transformation matrix relating the drift-output beam noise quantities to their input values is derived. With the circuit wave in synchronism with the space-charge waves, the excitation of the three synchronous waves and the two cyclotron waves is evaluated at the interaction input plane for a given impressed electric field on the circuit E_z and for each one of the beam noise quantities σ_1, y_1, v_y, and v_z. The cyclotron-wave excitation in comparison with that of synchronous waves is found to be negligibly small. It is shown that the velocities excite the synchronous waves very little when compared with the excitation due to E_z, σ_1, and y_1. Thus the analysis reduced to three-wave theory is adequate to describe the noise-figure behavior of space-charge wave amplifiers. Expressions for the noise figures of forward- and backward-wave amplifiers are derived. A scheme based on the small-signal interaction theory and the experimental noise-figure variation with beam position in the interaction space is proposed to determine the noise quantities and their correlations at the potential minimum.

By comparing the flow characteristics of the beam produced by the Kino short gun, Charles gun, and the

modified long gun with the Brillouin conditions, it is shown that the Kino short gun is capable of producing a nearly laminar beam. The conditions for maintaining a focused beam in the experimental tube are discussed. An experimental technique that resulted in repeatable noise-figure measurements is described.

Noise-figure reduction with decreasing diocotron gain is established and a method of achieving significant reduction in diocotron gain is proposed. The space-charge loading of the cathode in short guns is found to smooth cathode fluctuations and to result in a significant reduction in noise figure. On the contrary, space charge is found to enhance the noise from the modified long gun. The initial beam position fluctuations are shown to make a dominant contribution to the noise figure of crossed-field amplifiers. The noise figure is observed to decrease by several decibels by launching the beam close to the circuit as against the midway position between circuit and sole electrodes. The space-charge parameter S is established to be a significant parameter of the noise figure of crossed-field amplifiers.

Finally, the conditions for low-noise operation are established to be the following: (1) the use of a well-focused beam, (2) reduction of the diocotron gain of the gun and drift regions to a minimum possible value, (3) full exploitation of magnetic and space-charge smoothing for maximum reduction of noise figure, (4) launching the beam very close to the circuit, (5) reducing the space-charge parameter S close to zero, (6) high power gain, and (7) minimizing the initial beam position fluctuations by reducing the cathode thickness. By combining optimum beam focusing, space-charge smoothing, and beam displacement, low noise figures of 10.5 db for the backward-wave amplifier and 18.4 db for the forward-wave amplifier have been obtained without using noise transducers. A better control of the above factors than was possible with the present experimental tube will result in still lower noise figures. With the noise transducing scheme added to the factors listed above, it should be possible to obtain extremely low noise figures as was done by Wadhwa and Van Duzer.

CATHODE REGION STUDIES

(R. Y. C. Ho, Professor T. Van Duzer, Dr. S. P. Yu)

The objective of this project is to construct a relatively simple space-charge feedback model to study the noise phenomena under the space-charge-limited condition in both long and short guns as a two-dimensional problem, from the viewpoint of the potential minimum instability.

Construction of feedback model:

We assume that an M-type diode originally operates under a stable and completely space-charge-limited condition, that is, there is a potential minimum in front of the cathode. Suppose that, from some instant, the cathode emits an excess perturbation current i_s with a full Maxwellian velocity distribution in the normal direction and a half Maxwellian velocity distribution in the normal direction in addition to the original steady current. Electrons with different initial velocities $(\dot{z}_0, \dot{x}_0)$ will traverse through different trajectories. The instantaneous increase of space charge density deepens the potential minimum, which then turns some critical electrons, which would otherwise go into the stream, back to the cathode. These critical electrons flow back from their critical planes with almost zero initial velocities. We assume that the original steady beam current does not change but in addition to it there is a hole flow from the critical planes, where critical electron flows are generated, to compensate for the lack of critical electrons under the perturbed condition. In this formulation it is then see that there are three groups of perturbation flows; emission perturbation current flow (a temperature-limited shot noise current), critical electron flow, and hole flow. Each perturbation flows along a different trajectory in the diode. Thus they form quite different Green's functions, which relate the perturbation flow to the potential minimum perturbation at some point in front of the cathode. We denote the Green's function of the pure shot-noise current, hole flow, and the critical electron flow as $G_s(z_1', z)$, $G_h(z', z)$, and $G_e(z', z)$, respectively, where z'

denotes the coordinate of the source point and z denotes the coordinate of the observation point.

The Green's functions were calculated for the case where the beam current $J_a = 2000$ amp/m^2, magnetic field B = 800 Gauss, the current sorting ration $J_a/J_s = 0.376$, the cathode temperature $T = 1160^\circ$ K, and the cathode length $l_k = 3.0 \times 10^{-4}$ m with the exit plane located far enough from the cathode such that all of the perturbation current flows contribute the maximum space charge, as shown in Fig. 7. It is seen from Fig. 7 that the curves of the Green's functions for different point z's are similar and they have translational symmetry since in the calculation, the maximum contributions of space charge are taken.

The potential minimum fluctuations for the same case but with the ratio of cathode length to the cycloid length equal to 0.5 and 0.6 are plotted in Figs. 8 and 9, respectively. It is seen from Fig. 8 that the fluctuations of the potential minimum are convergent to a steady value, that is, as a result of the introduction of an excess emission current density i_s, of long duration, into the M-type diode, it brings the system into a new equilibrium; however, from Fig. 9 the potential minimum fluctuation is divergent, that is, for this particular case the excess perturbation current i_s leads the system into instability.

The resultant average perturbation of the beam current density for the same case is calculated and also the shot-noise smoothing factors, as shown in Fig. 10. It is seen from Fig. 10 that when the cathode width is 0.6 times the cycloid length, instability is obtained; when the cathode width is less than 0.6 times the cycloid length, smoothing of shot noise current is obtained. When the cathode width is 0.25 times the cycloid length or less, the shot-noise smoothing factor is practically constant and attains the value for the ordinary diode.

Continuing this work we will proceed to study the effect of the magnetic field on potential minimum fluctuation with the cathode width fixed.

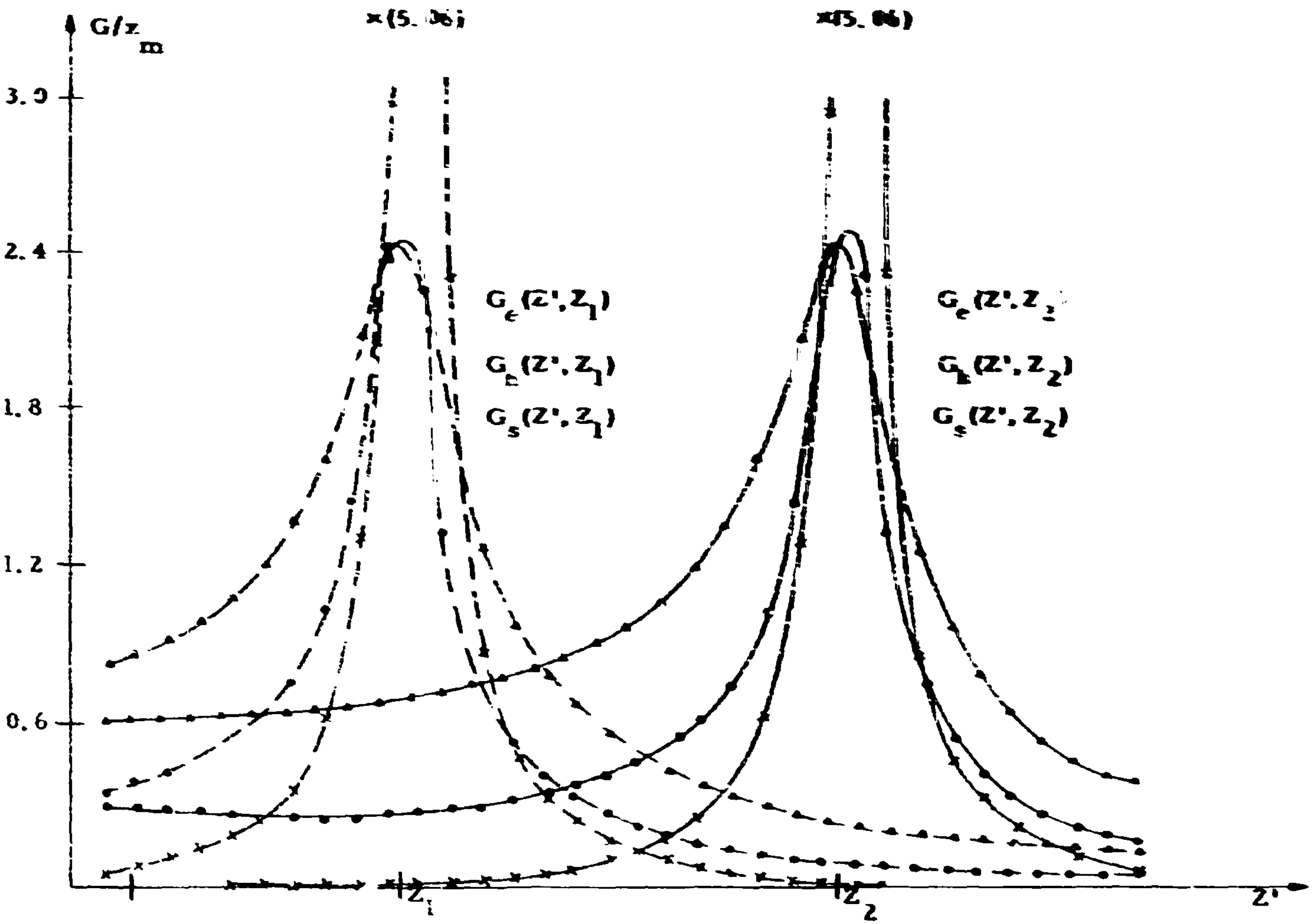

Fig. 7. Curves of the Green's functions for the different observation points.

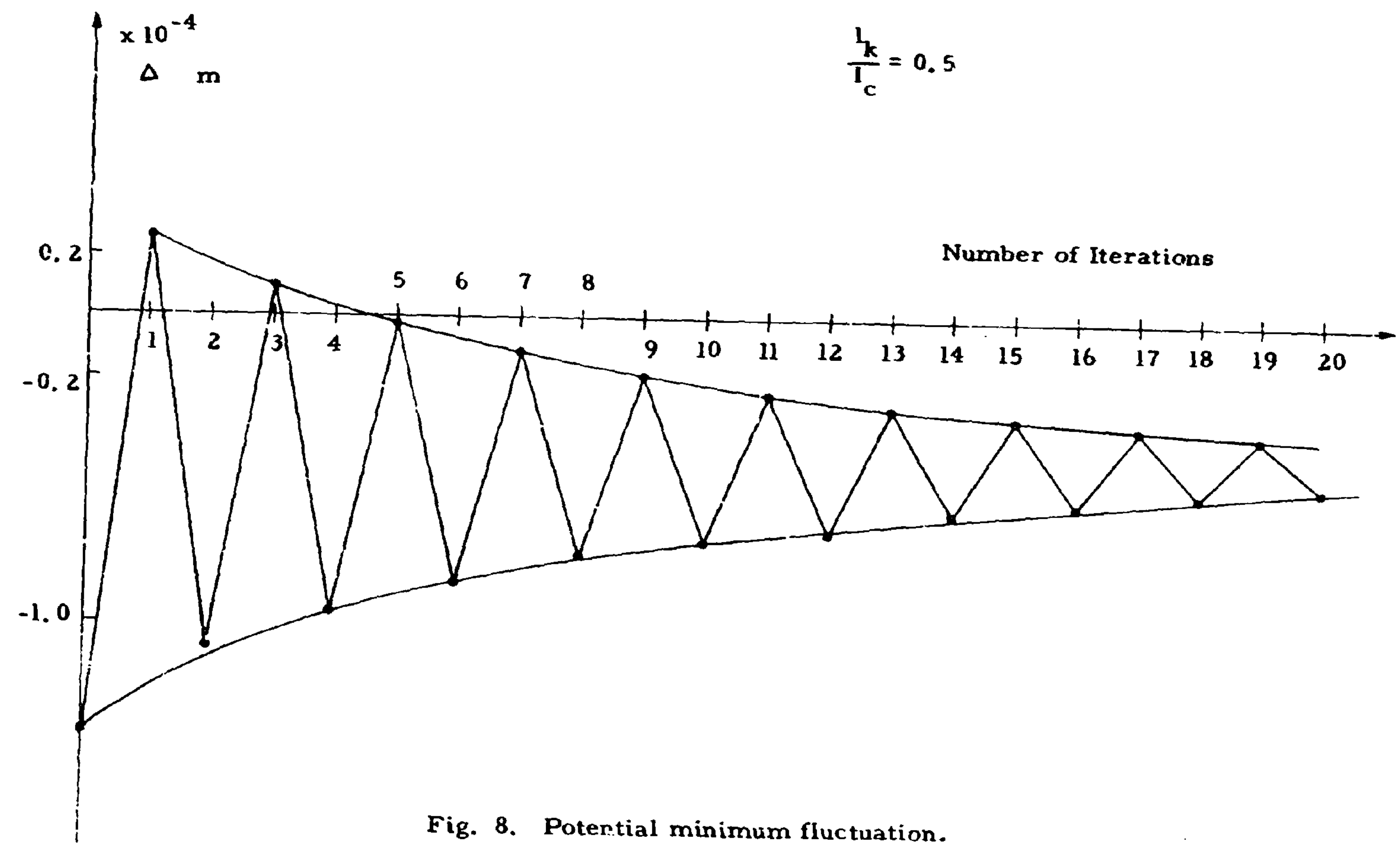

Fig. 8. Potential minimum fluctuation.

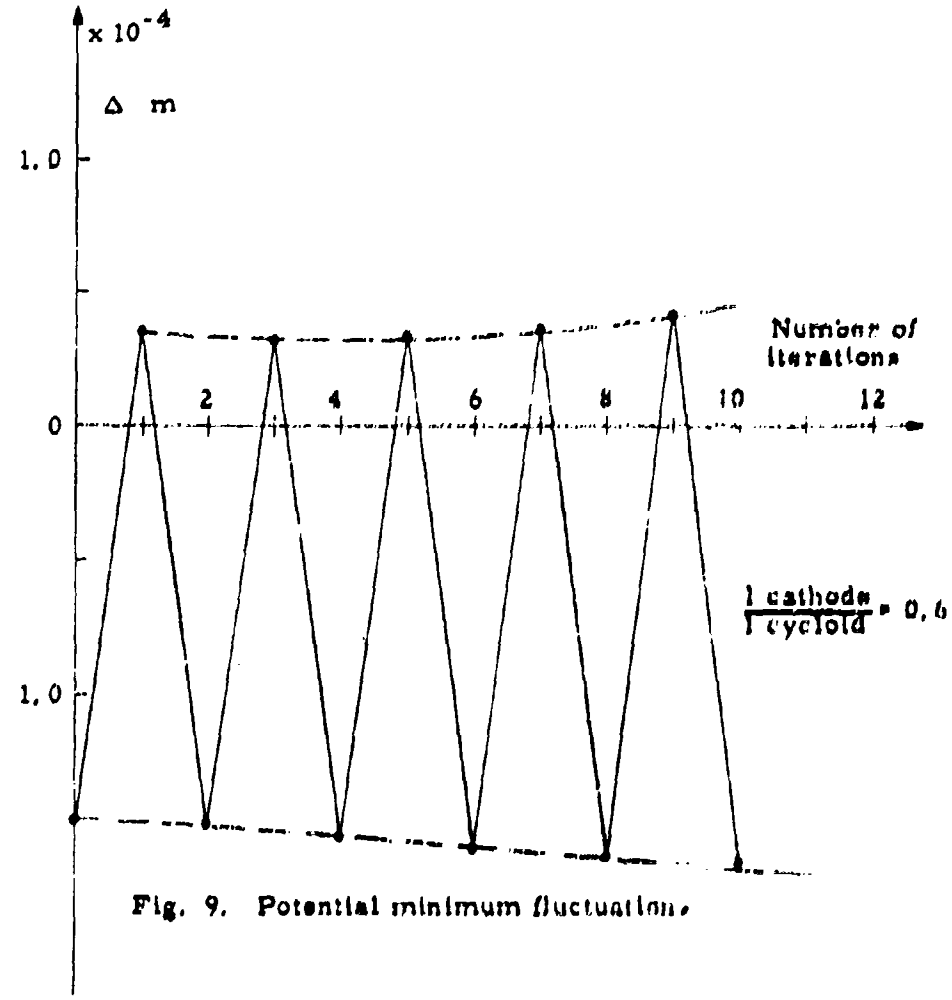

Fig. 9. Potential minimum fluctuation.

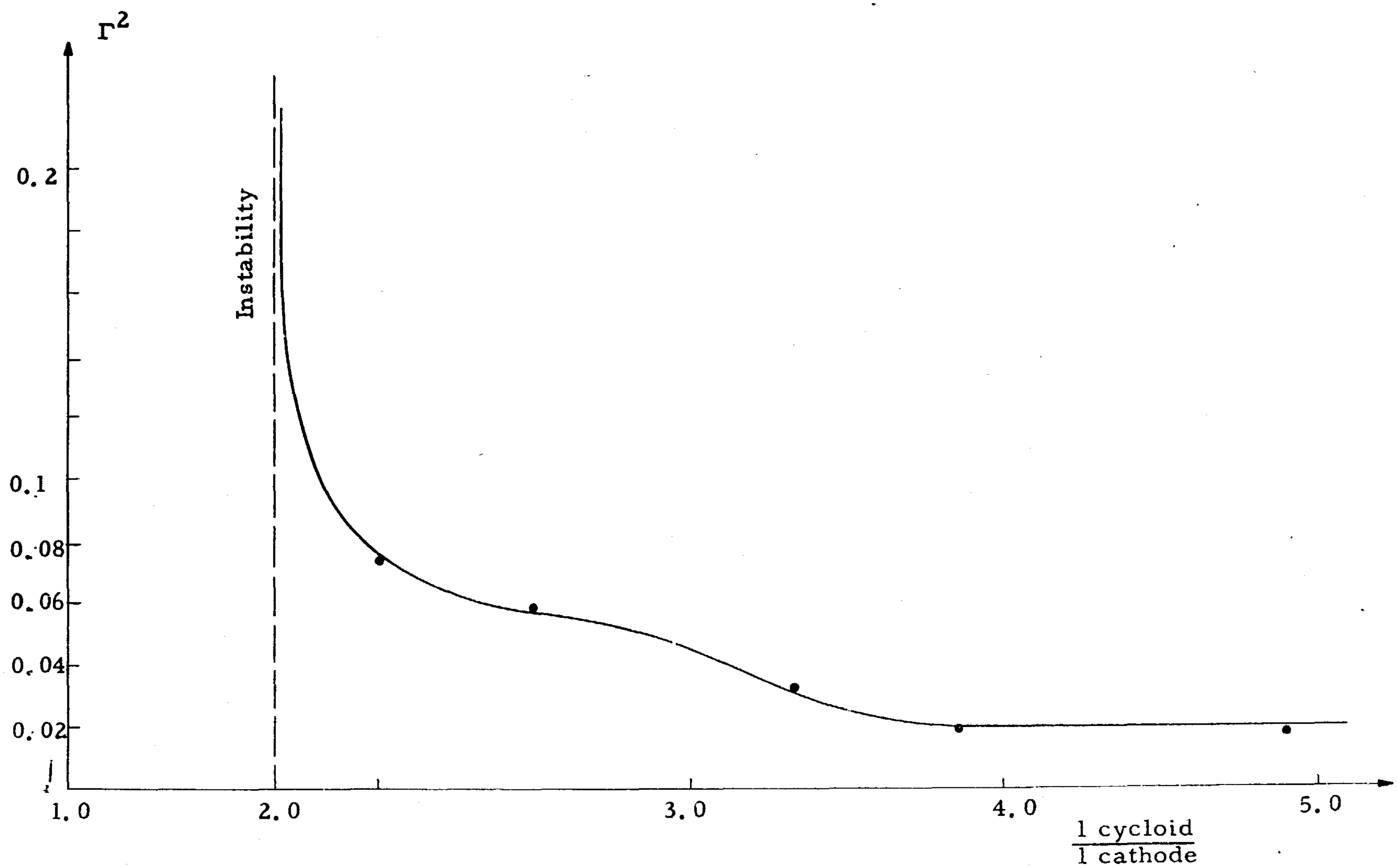

Fig. 10. Space charge shot noise factor versus the ratio of cycloid length to cathode length.

SECOND-ORDER CORRECTIONS TO THE FIRST-ORDER CROSSED FIELD SHEET BEAM FLOW

(G. A. Poe, Professor T. Van Duzer and Dr. S. P. Yu)

A first-order electron sheet-beam flow developed by Rao [1] has been studied and used to evaluate a second-order correction term to the first-order beamwidth. The second-order paraxial-ray formulation involves the plotting of a curvilinear coordinate system q_1 and q_2 where the q_1 = constant lines are approximated by circular arcs (see Fig. 11). This particular second-order coordinate system has been drawn and the beamwidths of the first and second-order flows plotted on the coordinate system.

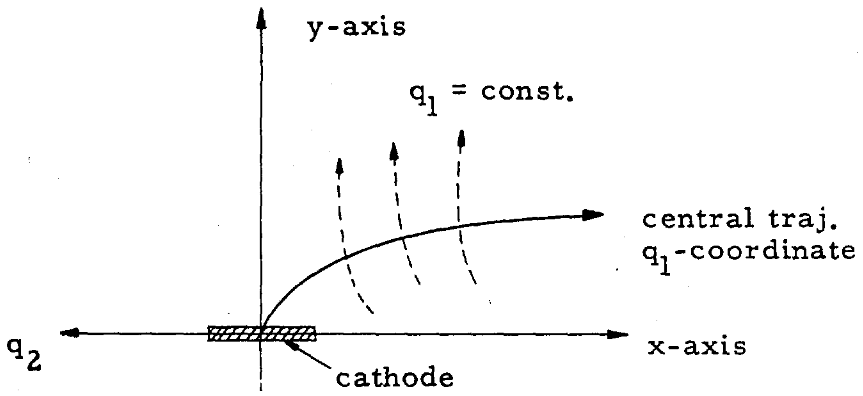

Fig. 11. Coordinate system used in the second-order flow.

The second-order beamwidth is defined as

$$\xi_1 q_{20} + \frac{1}{2}\xi_q q_{20}^2 , \tag{1}$$

[1] R. Rao, "Study of Crossed-Field Amplifiers," Ninth Quarterly Report, ERL, 16 June to 15 Sept. 1965.

where q_{20} is half the cathode width, $\mathring{\xi}_1$ is the first-order scale factor, and $\mathring{\xi}_q$ is the second-order scale factor.

The first-order beamwidth is defined as:

$$\xi_1 q_{20} \, . \tag{2}$$

Hence, one sees that the second-order correction term to the first-order flow is

$$\frac{1}{2} \xi_q q_{20}^2 \, . \tag{3}$$

For a q_{20} of one unit, the two beamwidths have been calculated and plotted in Fig. 12. The dashed line represents the first-order beamwidth and the solid line the second-order beamwidth. It is to be noted that the second-order correction term is very small for a cathode width of two units.

For a q_{20} of four units, the two beamwidths are shown in Fig. 13. The dashed line represents the first-order beamwidth and the solid line represents the second-order beamwidth. It is to be seen that the second-order correction term is significant in this large cathode case.

The next step in the project is to calculate the electrode structure that would produce the second-order flow and compare these electrodes with those calculated for the first-order flow.

CROSSED-FIELD INTERACTIONS OF EM AND SOUND WAVES WITH CURRENT CARRIERS IN SOLIDS

(M. Meyer, Professor J. R. Whinnery and Dr. S. P. Yu)

The prupose of this investigation is to find possible ways to use solids in static electric and magnetic fields to amplify EM waves.

A number of recent experiments, and some theory, indicate that it is possible to use the conduction electrons and/or holes in bulk solids to generate and amplify EM signals. The interactions in some

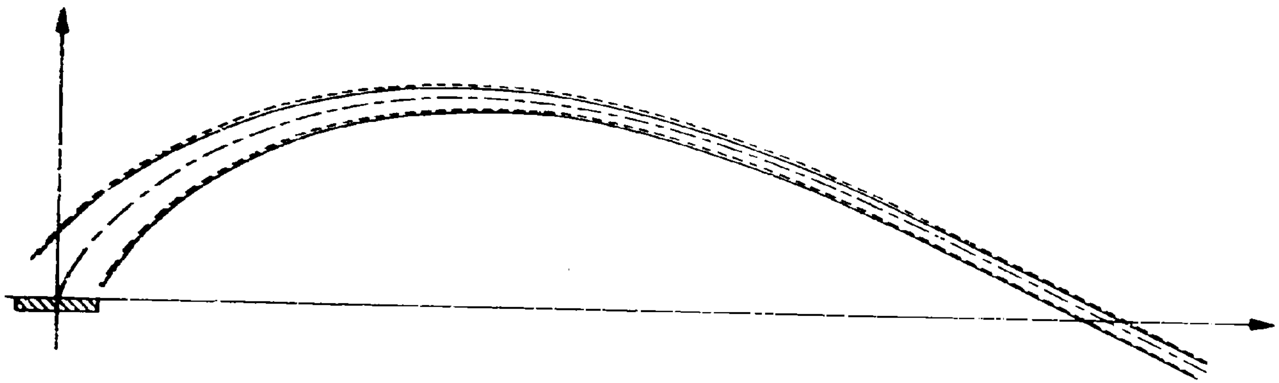

Fig. 12. Second-order and first-order Beamwidths for a cathode width of two units.

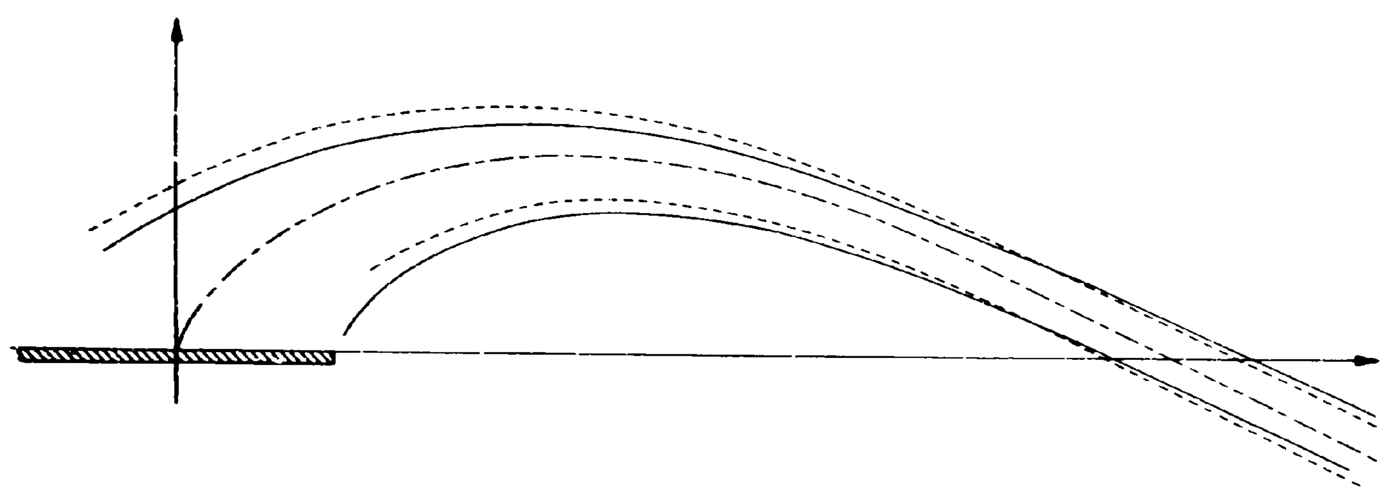

Fig. 13. Second-order and first-order Beamwidths for a cathode width of eight units.

cases can be considered analogous to that of a traveling wave tube. That is, electrons (say) are caused to drift through a solid by means of a dc electric field. When the drift velocity is near the phase velocity of an acoustic or EM wave in the solid, energy can be transferred between the wave and carriers.

In one study [1] a slow wave circuit is etched on the surface of a solid (InSb) carrying a direct current in the direction of the slow wave. The resulting interaction should amplify the wave.

Another case [2] is that of an ultrasonic wave propagated in the direction of current flow in semimetals. Here a dc magnetic field perpendicular to the dc electric field is necessary.

A third example is the helicon [3] wave which can propagate in a conductor provided there is a strong dc magnetic field present. Helicon waves can have very slow phase velocities, hence can interact with the rather slow electrons in a current-carrying conductor. To date, there have been no reports of successful helicon wave amplification.

So far the work has been restricted to study of the reported phenomenon. Major stress is now on the helicon-wave analysis. Experimental techniques are also being developed.

---

[1] L. Sclymar and E. A. Ash, "Some traveling wave interactions in semiconductors," (unpublished).

[2] W. P. Dumke and R. R. Hearing, "Ultrasonic amplification in semimetals," Phys. Rev., 126, 1974 (1962).

[3] R. Bowers and M. C. Steel, "Plasma effects in solids," Proc. IEEE, Vol. 52 (Oct. 1964).

Security Classification

DOCUMENT CONTROL DATA - R&D

(Security classification of title, body of abstract and indexing annotation must be entered when the overall report is classified)

1. ORIGINATING ACTIVITY *(Corporate author)*
University of California, Berkeley, California

2a. REPORT SECURITY CLASSIFICATION
UNCLASSIFIED

2b GROUP
N/A

3. REPORT TITLE
STUDY OF CROSSED-FIELD AMPLIFIERS

4. DESCRIPTIVE NOTES *(Type of report and inclusive dates)*
Tenth Quarterly Progress Report - 16 September - 15 December 1965

5. AUTHOR(S) *(Last name, first name, initial)*
Rao, R. A., Van Duzer, T., Yu, S. P., Poe, G. A., Sasaki, A., Mantena, N. R., Ho, R. Y., Susskind, C.

6. REPORT DATE	7a. TOTAL NO. OF PAGES	7b. NO. OF REFS
May 1966	31	12

8a. CONTRACT OR GRANT NO.
DA 36-039 AMC-02164(E)

b. Task No.

c.

d.

9a. ORIGINATOR'S REPORT NUMBER(S)

9b. OTHER REPORT NO(S) *(Any other numbers that may be assigned this report)*

10. AVAILABILITY/LIMITATION NOTICES This document is subject to special export controls and each transmittal to foreign governments or foreign nationals may be made only with prior approval of CG, USAECOM, Attn: AMSEL-KL-TM, Fort Monmouth, N. J.

11. SUPPLEMENTARY NOTES

12. SPONSORING MILITARY ACTIVITY
U. S. Army Electronics Command
Fort Monmouth, New Jersey AMSEL-KL-TM

13. ABSTRACT

An electron gun in which the cathode and accelerating regions are shielded from the magnetic field of the drift region is proposed. Beam synthesis techniques are utilized to obtain electrode configurations which produce a nearly laminar beam. Second order corrections to the beam synthesis method are found to be insignificant for the case of a large cathode width. Expression for the minimum noise-figure of crossed-field amplifiers is derived and its dependence on the space-charge parameter is shown.

The parametric dependence of the noise-figure of crossed-field microwave amplifiers was established theoretically and experimentally. Conditions for the low-noise operation of crossed-field amplifiers were obtained. The dependence of space-charge smoothing factor as a function of cycloid length to cathode length is estimated from the theoretical study of the crossed-field potential minimum region.

The study of certain crossed-field effects in solids was initiated.

DD FORM 1 JAN 64 1473

Security Classification

Security Classification

14. KEY WORDS	LINK A		LINK B		LINK C	
	ROLE	WT	ROLE	WT	ROLE	WT
Crossed-field amplifier Crossed-field guns Shielded gun Potential minimum instability Noise Minimum noise-figure Noise smoothing						

INSTRUCTIONS

1. ORIGINATING ACTIVITY: Enter the name and address of the contractor, subcontractor, grantee, Department of Defense activity or other organization *(corporate author)* issuing the report.

2a. REPORT SECURITY CLASSIFICATION: Enter the overall security classification of the report. Indicate whether "Restricted Data" is included. Marking is to be in accordance with appropriate security regulations.

2b. GROUP: Automatic downgrading is specified in DoD Directive 5200.10 and Armed Forces Industrial Manual. Enter the group number. Also, when applicable, show that optional markings have been used for Group 3 and Group 4 as authorized.

3. REPORT TITLE: Enter the complete report title in all capital letters. Titles in all cases should be unclassified. If a meaningful title cannot be selected without classification, show title classification in all capitals in parenthesis immediately following the title.

4. DESCRIPTIVE NOTES: If appropriate, enter the type of report, e.g., interim, progress, summary, annual, or final. Give the inclusive dates when a specific reporting period is covered.

5. AUTHOR(S): Enter the name(s) of author(s) as shown on or in the report. Enter last name, first name, middle initial. If military, show rank and branch of service. The name of the principal author is an absolute minimum requirement.

6. REPORT DATE: Enter the date of the report as day, month, year; or month, year. If more than one date appears on the report, use date of publication.

7a. TOTAL NUMBER OF PAGES: The total page count should follow normal pagination procedures, i.e., enter the number of pages containing information.

7b. NUMBER OF REFERENCES: Enter the total number of references cited in the report.

8a. CONTRACT OR GRANT NUMBER: If appropriate, enter the applicable number of the contract or grant under which the report was written.

8b, 8c, & 8d. PROJECT NUMBER: Enter the appropriate military department identification, such as project number, subproject number, system numbers, task number, etc.

9a. ORIGINATOR'S REPORT NUMBER(S): Enter the official report number by which the document will be identified and controlled by the originating activity. This number must be unique to this report.

9b. OTHER REPORT NUMBER(S): If the report has been assigned any other report numbers *(either by the originator or by the sponsor)*, also enter this number(s).

10. AVAILABILITY/LIMITATION NOTICES: Enter any limitations on further dissemination of the report, other than those imposed by security classification, using standard statements such as:

(1) "Qualified requesters may obtain copies of this report from DDC."

(2) "Foreign announcement and dissemination of this report by DDC is not authorized."

(3) "U. S. Government agencies may obtain copies of this report directly from DDC. Other qualified DDC users shall request through ________________."

(4) "U. S. military agencies may obtain copies of this report directly from DDC. Other qualified users shall request through ________________."

(5) "All distribution of this report is controlled. Qualified DDC users shall request through ________________."

If the report has been furnished to the Office of Technical Services, Department of Commerce, for sale to the public, indicate this fact and enter the price, if known.

11. SUPPLEMENTARY NOTES: Use for additional explanatory notes.

12. SPONSORING MILITARY ACTIVITY: Enter the name of the departmental project office or laboratory sponsoring *(paying for)* the research and development. Include address.

13. ABSTRACT: Enter an abstract giving a brief and factual summary of the document indicative of the report, even though it may also appear elsewhere in the body of the technical report. If additional space is required, a continuation sheet shall be attached.

It is highly desirable that the abstract of classified reports be unclassified. Each paragraph of the abstract shall end with an indication of the military security classification of the information in the paragraph, represented as *(TS), (S), (C), or (U)*.

There is no limitation on the length of the abstract. However, the suggested length is from 150 to 225 words.

14. KEY WORDS: Key words are technically meaningful terms or short phrases that characterize a report and may be used as index entries for cataloging the report. Key words must be selected so that no security classification is required. Identifiers, such as equipment model designation, trade name, military project code name, geographic location, may be used as key words but will be followed by an indication of technical context. The assignment of links, roles, and weights is optional.

DD FORM 1 JAN 64 1473 (BACK)

Security Classification